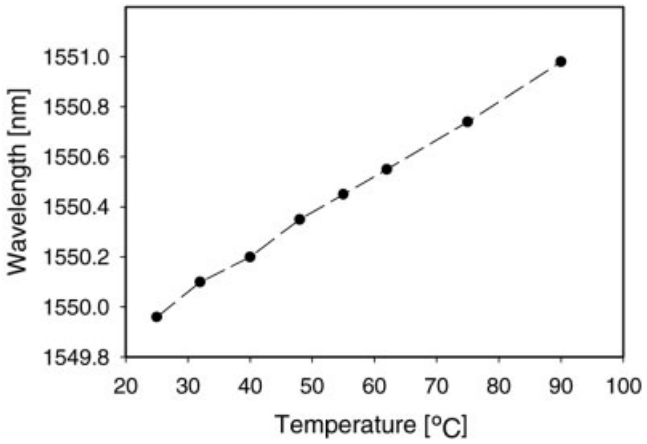

Figure 7 Wavelength tuning characteristics of the fiber laser

laser cavity. The FBG F-P etalon discriminates and selects the laser longitudinal modes efficiently. The spatial hole burning effect is restrained by using fiber Faraday rotator. The output power is more than 50 mW and slope efficiency is 27%. The linewidth of the fiber laser is less than 10 kHz. The temperature tuning results indicate the laser exhibits good stability. The fiber laser has a number of potential applications for high resolution fiber sensor.

REFERENCES

1. M. Horowita, R. Daisy, and B. Fischer, et al, Narrow-linewidth, single-mode Er-doped fibre laser with intracavity wave mixing in saturable absorber, Electron Lett 30 (1994), 648–649.
2. Y. Cheng, J.T. Kringlebotn, and W.H. Loh, et al, Stable single-frequency traveling-wave loop laser with integral saturable absorber-based tracking narrow-band filter, Opt Lett 20 (1995), 875–877.
3. S. Huang, Y. Feng, and J. Dong, et al, 1083 nm single frequency ytterbium doped fiber laser, Laser Phys Lett 2 (2005), 498–501.
4. D.I. Chang, M.J. Guy, and S.V. Chernikov, et al Single-frequency Er fiber laser using the twisted-mode technique, Electron Lett 32 (1996), 1786–1787.
5. G.A. Ball, W.W Morey, and W.H Glenn, Standing-wave single mode Er fiber laser. IEEE Photon Technol Lett 3 (1991), 613–615.
6. J.L. Zyskind, V. Mizahri, and D.J DiGiovanni, et al, Short single frequency Er-doped fibre laser, Electron Lett 28 (1992), 1385–1387.
7. M. Sejka, P. Varming, and J. Hübner, et al, Distributed feedback Er^{3+}-doped fibre laser, Electron Lett 31 (1995), 1445–1446.
8. C. Spiegelberg, J. Geng, and Y. Hu, et al, Low-noise narrow-linewidth fiber laser at 1550 nm, Lightwave Technol 22 (2004), 57–62
9. Y. Kaneda, C. Spiegelberg, and J. Geng, et al, 200-mW, narrow-linewidth 1064.2-nm Yb-doped fiber laser, Paper presented at Lasers and Electro-Optics Conference (CLEO), 2004, 2, CTh03:1–2.
10. H. Ludvigsen, M. Tossavainen, and M. Kaivola, Laser linewidth measurements using self-homodyne detection with short delay, Opt Commun 155(1998), 180–186.

A BAND-PASS FILTER USING VIA-HOLE-WALL CAVITY

Ruey Bing Hwang and Jun Liang Pan
Department of Communication Engineering, National Chiao Tung University, Hsinchu, Taiwan, Republic of China

Received 23 October 2006

ABSTRACT: *In this paper, we presented a band-pass filter consisting of a post-wall cavity resonator. This band-pass filter was fabricated in a two-layered printed circuit board, which includes an input and an output substrate integrated waveguides as the feeding structures in the top layer and a cavity in the bottom layer. The interconnection of the signal between different layers is achieved via the apertures etched on the input and output waveguides and cavity. We found the bandwidth of such a class of band-pass filter could be altered by tuning the length of the coupling apertures. Besides, the pass-band frequency can be estimated by the resonant frequencies of the cavity. We have fabricated the band-pass filter on a low-loss dielectric substrate and measured its S-parameters, including the return- and insertion- loss. In addition, the numerical simulation by the CST microwave studio, a full-wave time-domain numerical method, was also carried out. A good agreement between the measured and simulation results was obtained.* © 2007 Wiley Periodicals, Inc.
Microwave Opt Technol Lett 49: 1456–1459, 2007; Published online in Wiley InterScience (www.interscience.wiley.com). DOI 10.1002/mop.22438

Key words: *via-hole-array waveguide; periodic structures; band-pass filter*

1. INTRODUCTION

Recently, the via-hole-wall (or post-wall) technique [1–8], or the substrate integrated waveguide technique [1–4], was developed to fabricate an equivalent rectangular metallic waveguide or cavity on a PCB (printed circuit board) with low-loss dielectric substrate. Such a class of waveguides has been proved [2] to be able to preserve the well-known advantages of commonly used closed rectangular waveguide, such as high-Q factor. Besides, the substrate integrated waveguide is based on PCB fabrication process; therefore, it is easy for being integrated with the micro-strip, coplanar waveguide, or the other planar circuits, to design a microwave/mm wave sub-system. In addition to the substrate integrated waveguide, the cavity based on the via-hole-wall technology was also well developed [3]. The novel substrate integrated waveguide cavity filter with defected ground structure was investigated to provide a high stop-band rejection and low insertion loss. The V-band 3-D multilayer cavity resonators and three-pole (three coupling cavities) band-pass filters using slot excitation with quarter guided-wave wavelength open stub was demonstrated [9].

In this paper, we developed a band-pass filter using a cavity resonator with two coupling apertures. The cavity resonator was fabricated using via-hole array to approximate the metal wall. As was well known, when the pitch between two via holes is small enough, the via-hole array can act as a metallic wall to reflect the incident wave. Therefore, the electromagnetic field energy can be preserved within the cavity. Furthermore, the cavity feeding structure is a substrate integrated waveguide connecting with a taper micro-strip transition. The input/output substrate integrated waveguide is on the top of the cavity with their apertures overlapping to each other. Thus, the electromagnetic field coupling is taking place between the substrate integrated waveguide and the cavity resonator.

Since the band-pass filter is designed based on the cavity resonator, the pass-band frequency can be roughly estimated by its

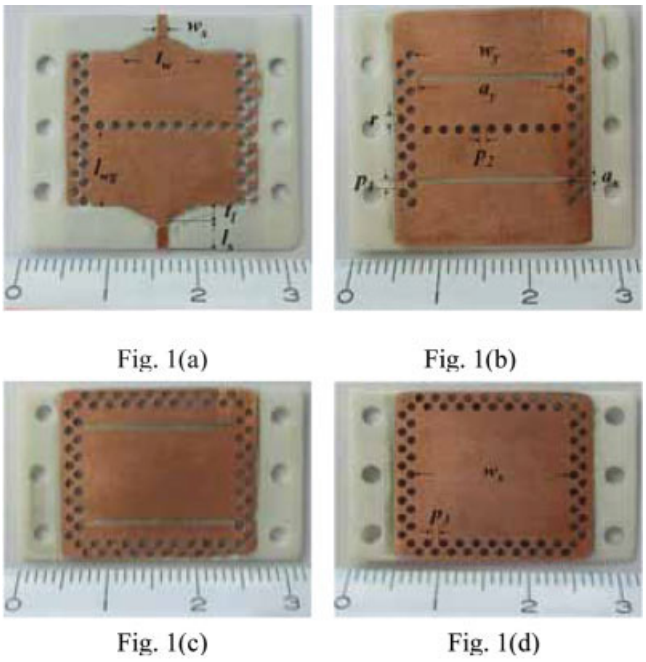

Figure 1 Structure configuration for the band-pass filter presented in this paper: (a) first layer (top side) including two via-hole-wall waveguides; (b) bottom side; (c) top side of the second layer including two coupling apertures in the resonant cavity; and (d) bottom side of the resonant cavity. [Color figure can be viewed in the online issue, which is available at www.interscience.wiley.com]

resonance frequency. As far as the resonance mode is concerned, the positions of excitation and probing affect the transmission response of the structure. Therefore, the positions of the two coupling aperture have to be properly designed to achieve a good performance in insertion loss. Besides, we found that the bandwidth of the band-pass filter can be altered by changing the length of the aperture. The detail information will be given in the following sections.

2. STATEMENT OF THIS PROBLEM

As shown in Figure 1, this band-pass filter consists of two dielectric layers; the top layer contains the input and output via-hole-wall waveguides and the bottom layer contains a via-hole-wall cavity. The electromagnetic field coupling between the via-hole-wall-waveguide and cavity is through the two apertures etched on the top surface of the cavity, and on the bottom surface of the waveguides, as well. The two input waveguides was isolated by placing the via-hole array between them. Notice that the pitch of the via-hole array separating the input and output waveguides should be kept as small as possible for preventing the direct coupling between the two waveguides. Besides, the input and output via-hole-wall waveguides are fed, respectively, by the micro-strip line with linear taper transition. The waveguide side walls or cavity walls are made from the double rows of via-wall to reduce the electromagnetic wave leakage. The parameters designated for the structure, shown in Figure 1, are listed in Table 1, with their size given in the second column.

3. EXPERIMENTAL AND NUMERICAL RESULTS

In this paper, the theoretical analysis for the scattering characteristics, including the insertion- and return- loss, was carried out using CST Microwave Studio®, based on the Finite Integration Technique (FIT) in time domain. Besides, the band-pass filter was

TABLE 1 Structure Parameter

Radius of via hole: r	0.5 mm
Width of waveguide (cavity width): w_y	17 mm
Via-hole array (waveguide wall) pitch: p_1	1 mm
Via-hole array (partition wall) pitch: p_2	0.55 mm
Via-hole array pitch (the second row): p_3	0.8 mm
Aperture length: a_y	17 mm
Aperture width: a_x	0.6 mm
Input/output waveguide length: l_{wg}	7.3 mm
Cavity length: w_x	17 mm
Micro-strip line width: w_s	1.2 mm
Micro-strip line length: l_s	3 mm
Taper transition width: t_w	9 mm
Taper transition length: t_l	1.7 mm

fabricated using microwave substrate RO4003 with thickness 20 mil. The via-hole arrays were implemented using electronic plating technique. In addition, the scattering parameters were measured by HP 8722D.

Figure 2 depicts the insertion- and return loss of the band-pass filter developed in this paper. The two coupling apertures share the same width and length, which are 0.6 mm and 17 mm, respectively. The length, width, and thickness of the resonance cavity are 15, 17, and 0.508 mm, respectively. The dashed lines denote the calculated result, while the solid lines represent the measured result. Since the thickness of the cavity is far smaller than the width and length, the major component of the electric field in the cavity is E_z, while E_x and E_y are negligible. Therefore, the lowest resonant mode is TM_{110} in this example. The resonant frequency for the (m, n, o) mode of the cavity without apertures is given below

$$f\,(\text{in GHz}) = 150\sqrt{(m/w)^2 + (n/l)^2}/\sqrt{\varepsilon_s}. \tag{1}$$

where the integer m and n denote the index number along width and length direction, respectively. The relative dielectric constant of the substrate is characterized by ε_s. However, because of the existence of two coupling apertures, the resonance frequency

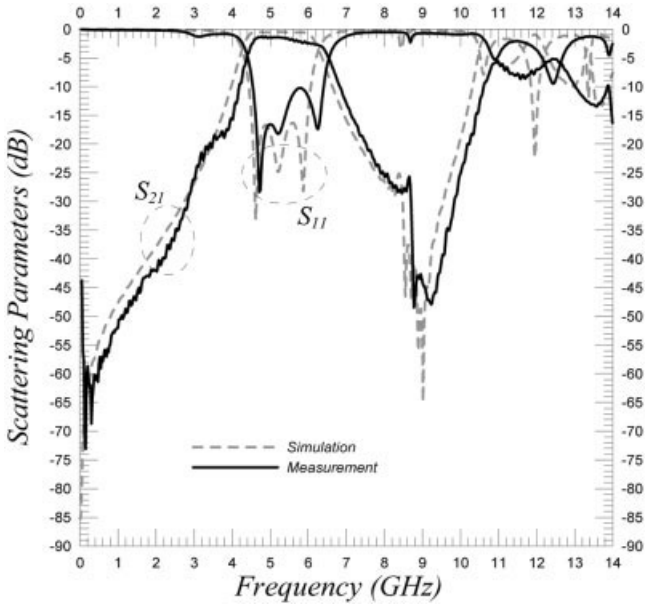

Figure 2 Measured and calculated insertion- and return-loss for the band-pass filter with aperture length 17 mm

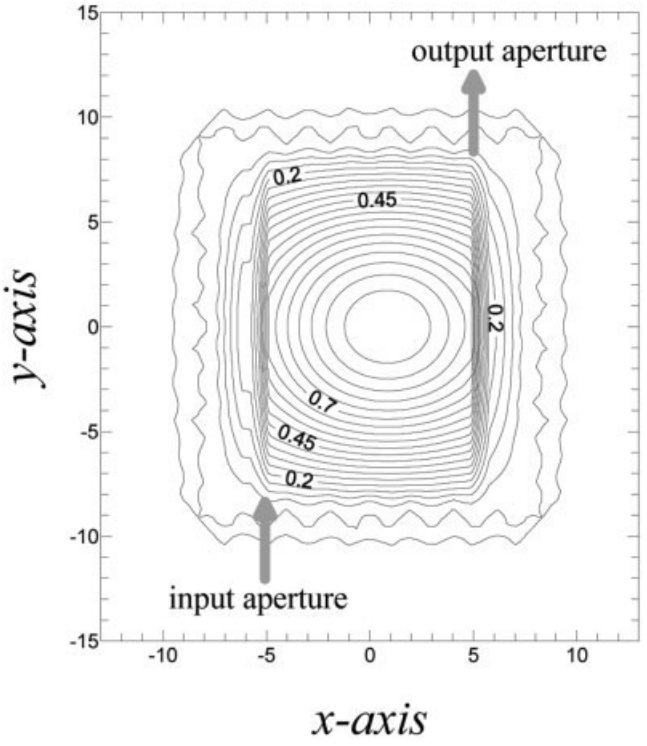

Figure 3 Distribution of the field contour (E_z component) inside the resonant cavity over the cross section at the position $z = 0.5h$, where h is the thickness of the substrate

should be different with the value given in (2). From Figure 2, it is obvious to see that the excellent agreement between the calculated and measured results.

As mentioned earlier, the band-pass characteristics of this filter is based on the resonance effect of the cavity. To prove that the band-pass characteristic is due to the resonant mode, TM_{110}, we plot the contour map, depicted in Figure 3, for the vertical component of electric field strength (E_z) on the cross section at $z =$

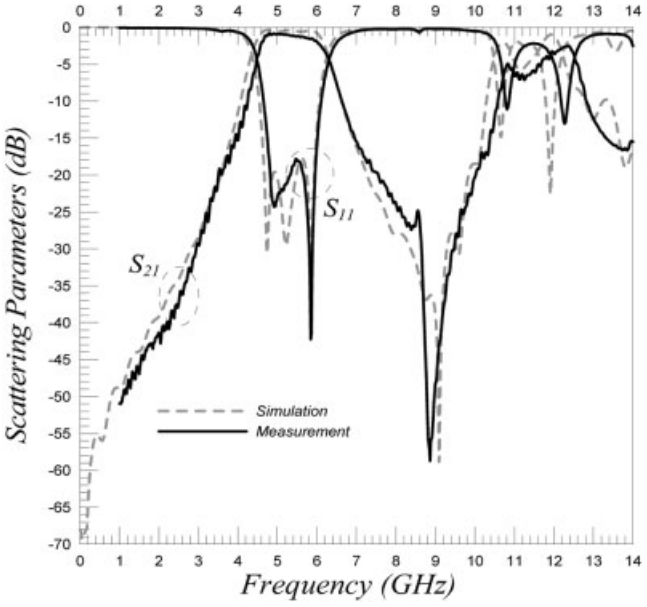

Figure 4 Measured and calculated insertion- and return-loss for the band-pass filter with aperture length 15 mm

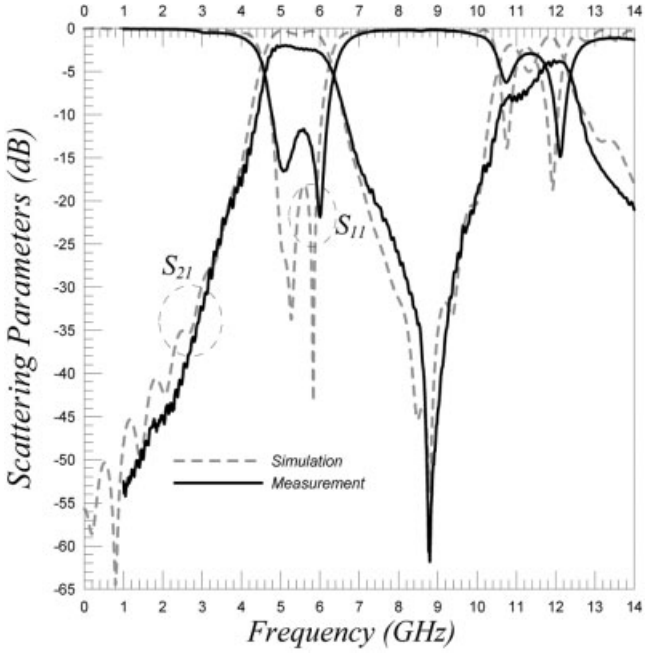

Figure 5 Measured and calculated insertion- and return-loss for the band-pass filter with aperture length 13 mm

$0.5h$ (h is the thickness of the substrate). From this Figure, it is apparent that the maximum electric field is around the center of the cavity and the field variation resembles the function given below.

$$E_z(x, y) \approx \sin\frac{\pi x}{w_x}\sin\frac{\pi y}{w_y}. \tag{2}$$

In the following two examples, we change the aperture length while keeping all the other parameters given in the previous example. The lengths of the aperture are 15 and 13 mm in Figures 4 and 5. Comparing Figures 4 and 5 with Figure 2, it is apparent that the bandwidth is decreasing as the aperture length is decreased. It is noted that the insertion loss in Figure 5 increases, compared with those in Figures 2 and 4. It may be conjectured that because of the decrease in the length of coupling aperture the coupling coefficient between the waveguide and cavity decreases accordingly. The bandwidth of the three cases shown in Figures 2, 4, and 5 are 34.05%, 30.28%, and 24.4%, respectively. Although not shown here, we have also carried out the numerical simulations and experimental studies for the cases with several different aperture lengths. We found that the bandwidth decreases as the decrease in the aperture length, however, the insertion loss increases.

4. CONCLUDING REMARKS

In this research, we developed a new band-pass filter using a resonant cavity, which is implemented by the via-hole-wall technique. The resonant cavity was coupled by an aperture on a substrate integrated waveguide stacked on the top of the resonant cavity. Because of the vertical coupling between the substrate integrated waveguide and cavity, the size of the structure is further reduced. Specifically, the bandwidth of this band-pass filter can be changed by tuning the length of the coupling aperture. Because of the easy fabrication and compact size, this band-pass filter can be a potential candidate in the microwave and millimeter wave system.

ACKNOWLEDGMENT

This research work was sponsored by Ministry of Education and National Science council, Taiwan, Republic of China.

REFERENCES

1. Z.C. Hao, W. Hong, X.P. Chen, J.X. Chen, K. Wu, and T.J. Cui, Multilayered substrate integrated waveguide (MSUBSTRATE INTEGRATED WAVEGUIDE) elliptic filter, IEEE Microwave Wireless Component Lett 15 (2005), 95–97.
2. Feng Xu and Ke Wu, Guided-wave and leakage characteristics of substrate integrated waveguide, IEEE Trans Microwave Theory Technol 53 (2005), 66–73.
3. Y.L. Zhang, W. Hong, K. Wu, J. Xin, Chen, and H.J. Tang, Novel substrate integrated wavegudide cavity filter with defected ground structure, IEEE Trans Microwave Theory Technol 53 (2005), 1280–1287.
4. J. Papapolymerou, J. Cheng, J. East, and L. Katehi, A micromachined high-QX-band resonator, IEEE Microwave Guided Wave Lett 7 (1997), 168–170.
5. M.J. Hill, R.W. Ziolkowski, and J. Papapolymerou, Simulated and measured results from a duroid-based planar MBG cavity resonator filter, IEEE Microwave Guided Wave Lett 10 (2000), 528–530.
6. W.J. Chappell, M.P. Little, and L.P.B. Katehi, High isolation, planar filters using EBG substrates, IEEE Microwave Wireless Component Lett 11 (2001), 246–248.
7. H.J. Hsu, M.J. Hill, R.W. Ziolkowski, and J. Papapolymerou, A duroid-based planar EBG cavity resonator filter with improved quality factor, IEEE Antennas Wireless Propag Lett 1 (2002), 67–70.
8. H.J. Hsu, M.J. Hill, J. Papapolymerou, and R.W. Ziolkowski, A planar X-band electromagnetic bandgap (EBG) 3-pole filter, IEEE Microw Wireless Component Lett 12 (2002), 255–257.
9. J.-H. Lee, S. Pinel, J. Papapolymerou, J. Laskar, and M.M. Tentzeris, Low-loss LTCC cavity filters using system-on-package technology at 60GHz, IEEE Trans Microwave Theory Technol 53 (2005), 3817–3824.
10. N. Marcuvitz, Waveguide handbook, McGraw-Hill, New York, 1951.

DOUBLE-LAYER SUBSTRATE INTEGRATED WAVEGUIDE STRUCTURE WITH VARIABLE FRACTIONAL BANDWIDTH

Lei Xu, Wenquan Che, Liang Geng, and Dapeng Wang
Department of Electrical Engineering, Nanjing University of Science and Technology, 210094 Nanjing, China

Received 28 October 2006

ABSTRACT: *The propagation characteristics of double-layer SIW structures have been investigated in this paper. On the basis of the theory of resonance cavity and SIW, the simple theoretical formulas for the lower and upper frequencies in the passband have been found. The theoretical analyses have indicated that these two frequencies have much dependence on the width of SIW and the length of the coupling slot, the fractional bandwidth of the double-layer SIW structures can be controllable. Agreement between the simulation data and the calculated results from the formulas can be observed.* © 2007 Wiley Periodicals, Inc. Microwave Opt Technol Lett 49: 1459–1463, 2007; Published online in Wiley InterScience (www.interscience.wiley.com). DOI 10.1002/mop.22469

Key words: *substrate integrated waveguide (SIW); double layer structures; propagation characteristics; controllable fractional bandwidth*

1. INTRODUCTION

In multilayer microwave integrated circuits such as low-temperature co-fired ceramics (LTCCs) or multilayer printed circuit boards (PCBs), waveguide-like structures can be fabricated in planar form by using periodic metallic via holes called *substrate-integrated waveguides* [1, 2]. The substrate-integrated waveguide structures can largely preserve the well-known advantages of conventional rectangular waveguides, viz., high Q and high power capacity, while they take the advantages of microstrip lines, such as low profile, small volume and light weight etc, it is useful for the design of millimeter-wave circuits such as filters, resonators, and antennas etc., [3–9]. In addition, it can easily be connected to microstrip or coplanar circuit using simple transitions [2, 3], which may lead to the design and development of compact low-loss millimeter-wave integrated circuits and systems. Such developments should enhance manufacturing repeatability, reliability, and cost reduction significantly. The advent of LTCC and multilayer circuit board makes it important to understand and analyze with simplicity the characteristics of substrate-integrated waveguide structures. Some empirical formulas of the equivalent rectangular waveguide width of the substrate-integrated waveguide have been given [3, 10]. The formulas indicate that the substrate-integrated waveguide structure has many similar properties as the conventional rectangular waveguide and the SIW structures can thus been analyzed as a rectangular waveguide with an equivalent width using typical waveguide theory. In addition, the equivalence of substrate-integrated waveguide to rectangular waveguide is done by an approach called as "*analytical* MoM" [11, 12], from which the width and length equivalence formulas have been found. Some experimental verification has been carried out, demonstrating the validity of the equivalence formulas.

For the sake of compactness and highly integration, double-layer and even multi-layer SIW structures are usually employed as the design platform for many microwave/mm wave devices and systems. Therefore, the propagation characteristics of double-layer SIW structures are investigated in this paper. The simple theoretical formulas for the lower and upper frequencies in the band of interest have been found. The analyses indicate that the fractional bandwidth of the double-layer SIW structure can be controllable; the lower and upper frequencies can be adjusted separately. Agreement can be observed between the measured data from the fabricated prototype and the calculation results, as well as the HFSS simulations, demonstrating the validity of the theoretical formulas.

2. ANALYTICAL FORMULAS

Unlike the conventional rectangular waveguide, only TE_{n0} modes can exist in the SIW structures because of the periodic cylinders forming the sidewalls of the SIW structure [10]. In addition, the dominant mode is still TE_{n0} mode. The schematic structure of SIW is shown in Figure 1. In the fundamental TE_{10} mode, the width equivalence between widths $a \ll$ and a, of substrate integrated rectangular waveguide and rectangular waveguide was derived as follows [11, 12]:

$$a' = \frac{2a}{\pi} \operatorname{arcctg}\left(\frac{\pi W}{4a} \ln \frac{W}{4R}\right) \tag{1}$$

Of which, W is the cylinder spacing and R, the radius of the cylinders forming the sidewalls of the SIW. With the formula, it is possible to find the equivalence width of the equivalent rectangular waveguide of SIW, and the SIW can thus be analyzed using typical RW theory, both having nearly the same propagation characteristics. As we know, the multilayer technology is the potential solu-